A Critical Compilation of Atomic Transition Probabilities for Singly Ionized Argon

V. Vujnović

Institute of Physics of the University, P. O. Box 304, 41001, Zagreb, Croatia

and

W. L. Wiese

National Institute of Standards and Technology, Gaithersburg, MD 20899, U.S.A.

Received March 27, 1992; revised manuscript received June 3, 1992

We have critically compiled the atomic transition probabilities of Ar II lines by combining recent high-accuracy lifetime data with branching-ratio emission measurements. We present several comparisons of the various literature data, including theoretical results, and we discuss our assessment procedure in detail. On the basis of this procedure, we present an extensive list of critically evaluated transition probabilities with uncertainty estimates.

Key words: argon; atomic transition probabilities; critically evaluated data; energy level data; wavelength data.

Contents

List of Tables

List of Figures

1. Introduction

Argon plasmas are widely used for fundamental plasma spectroscopy studies as well as for numerous applications involving technical plasmas, such as gas lasers and spectrochemical investigations with inductively coupled plasmas (ICPs). Thus the requisite spectroscopic data for Ar I and II—principally atomic transition probabilities and lifetimes of various energy levels—have been the subject of numerous investigations. Nevertheless, appreciable discrepancies have remained in the published data.

For Ar II, an opportunity has opened up to assemble an accurate set of transition probability data on the basis of recent high-accuracy lifetime data and of comprehensive good-quality branching ratio measurements, as well as a new advanced atomic structure calculation. We have critically evaluated these data, intercompared them and compiled a comprehensive table, also including reliable older data. We present this assembled table of absolute transition probability data with a critical discussion in this paper.

We should note that for Ar I, consistency of most emission data has been also recently achieved through a critical re-analysis of the data and by utilizing newly available

atomic lifetime data. Thus, a unified set of Ar I transition probabilities incorporating these advances has been proposed, too.[1]

2. Scope

The first extensive compilation of atomic transition probabilities for Ar II lines was undertaken by Wiese *et al.*[2] in 1969, who tabulated 240 transitions of the following transition arrays:

$$3s^2 3p^5 - 3s 3p^6 \qquad 3p^4 4s - 3p^4 4p$$
$$3p^5 - 3p^4 4s \qquad 3p^4 4p - 3p^4 4d$$
$$3p^4 3d - 3p^4 4p \qquad 3p^4 4p - 3p^4 5s$$

For the large majority of lines the uncertainties of these data were estimated to be typically in the range from $\pm 25\%$ to $\pm 50\%$. For the important $3d - 4p$ and $4s - 4p$ arrays, which give rise to many prominent lines in the visible and near UV spectrum, the uncertainties for the stronger lines were estimated to be normally within $\pm 25\%$.

Because of these relatively large uncertainties associated even with the prominent lines, and because of the increasing demand for more accurate data expressed by scientific and technical users, numerous new attempts to obtain improved data have been made since that time. Most of this work concerns the lines of the $3d - 4p$ and $4s - 4p$ transition arrays. This critical compilation therefore primarily addresses these two arrays, but also part of the $4p - 4d$ array.

For the wavelength and energy level data we have utilized the comprehensive measurements and analysis of Norlén,[3] which is entirely based on interferometric measurements, as well as the tables of Striganov and Odintsova.[4]

3. Data Assessment Procedure

Since 1970, the work on Ar II transition probability data has been carried out via three approaches:

(i) lifetime measurements;
(ii) emission measurements, especially branching ratio determinations; and,
(iii) quantum-mechanical calculations.

The central task in the critical compilation of literature data is the assessment of their quality and accuracy, since this determines the choice of the selected material. In order to accomplish this task in a consistent and objective manner, we have judged each paper by the following criteria, established in earlier critical tabulations[2]:

(1) a general evaluation of the capabilities and reliability of the applied experimental or theoretical method;
(2) the author's consideration of the major critical factors of his approach (see below) that enter into the results;
(3) the degree of agreement and general consistency between the author's results and other reliable data;
(4) the degree of fit of the data into established systematic trends and, if deviations exist, the reasons for such disagreements; and,
(5) the author's estimate of his uncertainties.

Very important are the "critical factors" mentioned in criterion (2). These factors concern the key problem areas in every approach and need to be taken care of in order to get accurate results. (Problem areas deemed of minor importance are not included.)

A. For lifetime experiments they are:
   1. Electron cascading from higher atomic levels;
   2. radiation trapping (self-absorption);
   3. collisional depopulation and repopulation; and,
   4. insufficient spectral resolution causing line blending.

B. For emission experiments the critical factors are:
   B.1. For "branching ratio" emission experiments:
      a. self-absorption;
      b. inadequate radiometric calibration procedures.
   B.2. For relative or absolute transition probability measurements in emission, additional critical factors are:
      c. line wing intensity and background intensity contributions;
      d. existence of partial or complete local thermodynamic equilibrium (LTE);
      e. inhomogeneities and boundary layers; and,
      f. inherent uncertainties in plasma diagnostic methods.

C. For quantum mechanical calculations, the following critical factors need to be taken into account:
   a. Electron correlation effects;
   b. severe cancellation in the transition integral; and,
   c. applicability of the adopted coupling scheme.

We have checked all papers for these critical factors and utilized for the final analysis those papers where all critical factors applicable to the particular type of investigation were adequately taken into account. Results of work in which these factors were only partially fulfilled, or not discussed, were either rejected for this analysis or, if no other data exist, were evaluated with great caution.

With respect to error estimates, we should note that the theoretically derived data carry no error estimates, since no reliable assessment of the uncertainties introduced by the various approximations into the calculations is possible. For experimental data — where error estimates may be readily made — we noticed that the un-

certainty statements sometimes are imprecise or incomplete, insofar as only statistical measurement errors have been listed without any estimate for systematic errors. It is therefore no surprise that numerous experimental results do not overlap within their mutual error estimates.

4. Transition Probability Data and Evaluation

4.1. Lifetime Measurements

As stated above, four critical factors must be considered in all lifetime experiments[2] which are:

(a) cascading;
(b) radiation trapping;
(c) collisional effects; and,
(d) insufficient spectral resolution.

The effects of radiation trapping and collision depopulation of an atomic level (factors (b) and (c)) are usually investigated and taken care of by varying the pressure in the observation chamber and thus the concentration of the species that is studied. If a systematic variation of the lifetime with pressure is seen, the pressure is reduced until no further variation in the lifetime is observed. Alternatively, if this point cannot be reached, extrapolation to zero pressure is undertaken. Factor (d), the possibility of insufficient spectral resolution, which causes lines to overlap, is normally taken care of by utilizing spectrometers with adequate resolving power.

This leaves the factor (a), i.e., electron cascading from higher excited atomic levels, which has been difficult to treat in some lifetime measurement techniques. This repopulation of the level to be studied has the effect of making the lifetime appear to be longer than it actually is. The selective excitation of specific atomic levels was probably first achieved in the early 1960s when atoms and ions were excited by electron beams of threshold energy so that no higher energy atomic states could be excited. Among the lifetime experiments available for Ar II, the work of Bennett *et al.*[5] and Garcia and Campos[6,7] falls into this category. In the mid-70's another cascade-free approach was applied to Ar II in the work of Camhy-Val *et al.*[8] and Mohamed *et al.*[9] These groups of authors observed coincidence signals from two successive radiative cascades. Their technique thus discriminates against all other radiative decays by registering only those events which occur through this two-cascade chain. The lifetime of the second of the two cascades may then be determined by this method. Also, when it was realized in the 70's that nonselective excitation in such techniques as beam foil spectroscopy and electron beam excitation at high energies had sometimes led to appreciable systematic errors, a new technique was devised to eliminate this error source. While curve fitting based on multi-exponential decays does not produce accurate results,[10] the technique utilizing "Arbitrarily Normalized Direct Cascades" (ANDC)[11] has been very successful. But, as the name implies, it requires the measurement of principal direct cascade levels. More recently, there has been the advent of tunable laser excitation,[12–15] where a pulsed laser is tuned to the transition of interest, thereby producing selective excitation and cascade-free radiative decay, sometimes referred to as laser induced fluorescence (LIF).

As usual, many transitions and levels of interest in Ar II are not directly connected to the ground state. In order to generate sufficient populations of these higher Ar II states, argon is excited in a strong discharge plasma so that singly charged ions are produced and a significant fraction of the ions are in these excited atomic levels. Laser pulses tuned to specific transition frequencies produce further selective excitations into higher levels from which the spontaneous decay is observed.

On the basis of the above discussion, one may thus group all lifetime experiments on Ar II into three distinctly different categories:

(a) experiments in which no radiative cascades occur, because the excitation is selective;
(b) experiments that contain cascade effects, which are however subsequently accounted for by an adequate correction technique. For example, this might be beam foil measurements with the ANDC technique or electron beam excitation experiments in which the electron energies are varied over an energy range that includes the threshold energy;
(c) experiments which are clearly nonselective in excitation and where the results have not been adequately corrected for radiative cascading.

The results of various lifetime experiments[6,9,13,14,16–26] from these three different categories clearly exhibit appreciable differences, as seen in Fig. 1 for the $4p\ ^4P^\circ_{5/2}$ level. (For completeness, Fig. 1 also contains the results of various theoretical approaches,[27–34] of which the work of Hibbert and Hansen,[34] shown by an open circle, is the most advanced.) Category (a) lifetime experiments, i.e., the two LIF experiments and a correlated photon experiment as well as an ANDC-corrected beam foil measurement, clearly show the least scatter (these are the data given as full circles). On the other hand, category (c) experiments, i.e., the other beam-foil experiments, the Hanle-effect measurement, the beam-gas and the delayed coincidence experiments, exhibit the largest scatter. In particular, the beam-foil experiments have a tendency to produce relatively long lifetimes as predicted. It should be noted again that the error estimates, given in Fig. 1 by the error brackets, are often too optimistic or might be incomplete, as seen by the numerous cases of non-overlapping results.

Since there are usually several results available for the transitions of interest, we have normally selected experiments of category (a) only. But for a few levels where no category (a) result was available, we utilized a category (b) experiment. In the following, only these experiments will be briefly discussed:

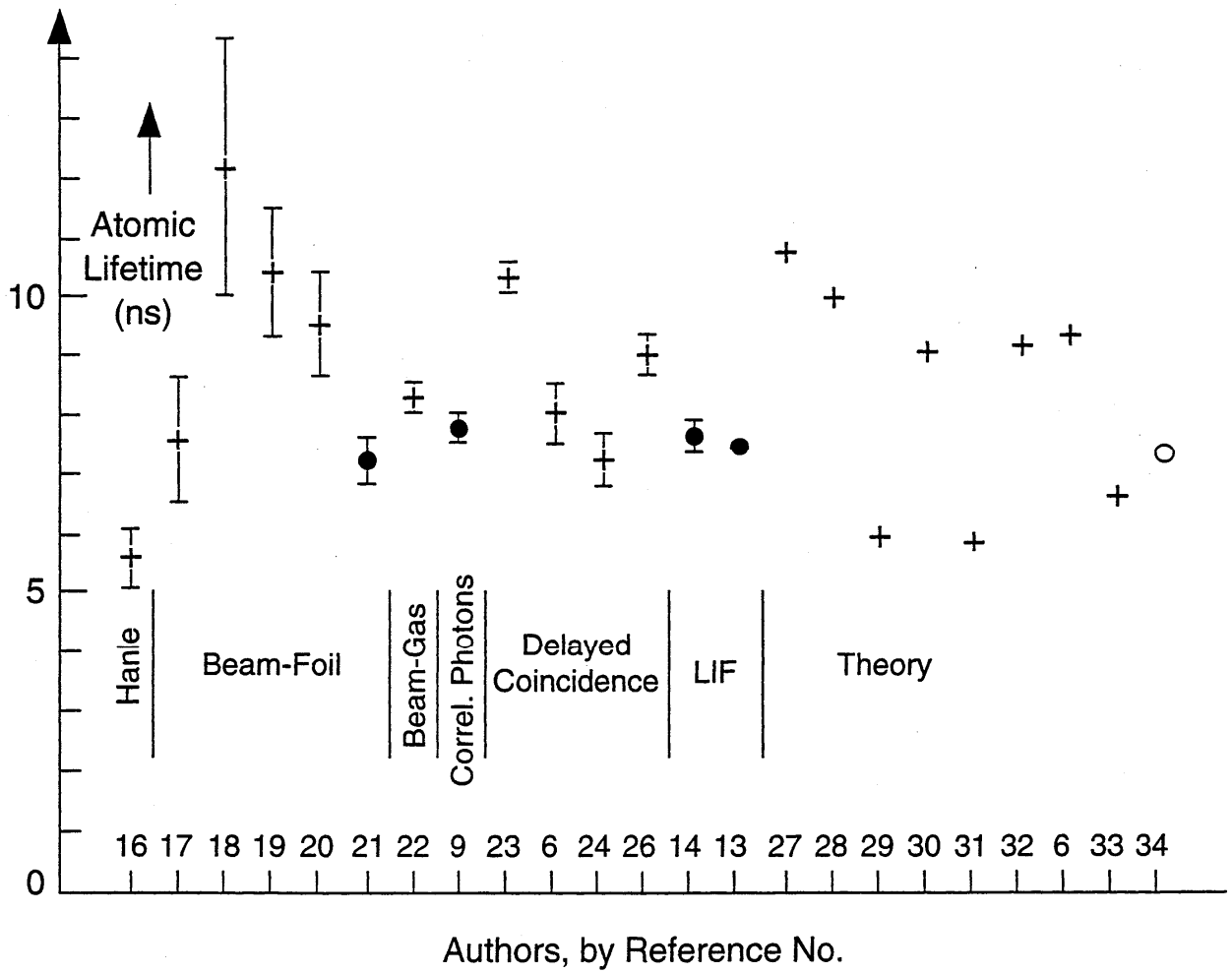

FIG. 1. Results of lifetime experiments and calculations for the $4p\ ^4P^\circ_{5/2}$ level. Full circles indicate experiments of highest quality, and the open circle an advanced calculation. Experiments are grouped according to techniques listed at the bottom. Reference numbers are shown on the x-axis. The uncertainties in the beam-laser (LIF) work by Schmoranzer *et al.*[13] are so small (about $\pm 1\%$) that they are not indicated.

Beam-Laser Experiments:

Three experiments have been reported since 1985 by Ward *et al.*,[12] Schmoranzer *et al.*[13] and Marger and Schmoranzer.[15] Fast monoisotopic ion beams have been generated at voltages of 30 ke$V$[12] and 162 ke$V$,[13,15] respectively. The ion beams were crossed perpendicularly with a mechanically chopped cw dye-laser which was tuned to the transition of interest. The spatial decay of the excited argon ions downstream from the beam-laser interaction region was recorded by means of a detector system that was accurately moved along the ion beam direction. With the precisely measured velocity of the fast ion beam, the length scale was converted to an accurate, highly resolved time scale,—as in beam foil experiments. An additional fixed detector system was applied as a monitor that normalized the magnitude of the detection signal. Radiation trapping effects were avoided by the very low density of the ion beam. Collisional quenching effects due to collisions with the residual gas were taken into account by measuring the effective lifetime at several gas pressures and extrapolating the decay rate to zero pressure. The influence of Zeeman quantum beats was eliminated with Helmholtz coils that compensate for the earth's magnetic field, and observations of the fluorescence photons were performed at the magic angle position of 54.7°. It should be noted that the latter effects and corrections were only discussed in the work by Schmoranzer and colleagues,[13,15] where further details and references are given.

Laser-excitation experiment:

In this type of experiment,[14] as in the above mentioned beam laser experiments, a tunable laser is used for selective excitation. However, in this case no fast ion beam is employed; the argon ions are generated in a pulsed dis-

charge, and individual time intervals for the re-emitted fluorescence radiation (delayed coincidences) are recorded and their statistical distribution is analyzed. The time resolution is typically not as high as in the beam laser technique with fast ion beams, and the accuracy is thus a bit less. Similar to the experiments above, tests have been made for the influence of radiation trapping and collisional quenching.

Electron beam threshold-energy excitation:

In 1964 Bennett *et al.*[5] measured the lifetimes of several Ar II levels by the delayed coincidence technique, employing a pulsed beam of threshold-energy electrons. Except for the different means of excitation, their technique is the same as for the above discussed lifetime work of Schade *et al.*[14] In order to test for possible collisional and radiation trapping effects, they varied the pressure in the discharge cell by a factor of 200, but did not observe any change in the lifetime. However, for some Ar^+ lines they reported line blending effects with neighboring neutral argon lines. They could separate the contributions of these lines due to the fact that their decay is much slower. Electron excitation close to threshold energies was also used by Garcia and Campos.[6,7]

4.1.a. Summary of Lifetime Results

In Table 1 we present the selected lifetimes ordered according to atomic level. A critical data assessment according to the criteria discussed earlier shows that the results of Schmoranzer *et al.*,[13] and Marger and Schmoranzer[15] are the most accurate ones, followed by an almost as accurate experiment by Ward *et al.*[12] When the results overlap, the agreement is very close. Also, the agreement is similarly good with the "cascade-free" measurements by Schade *et al.*[14] and Coetzer *et al.*,[21] considering that their results are estimated to be of somewhat larger uncertainty. (We should note that we generally apply two-standard deviations for the measurement errors (95% confidence limit), while some authors use one-standard deviations.) Other "cascade-free" lifetime results are available from the correlated-photon measurements of Camhy-Val *et al.*[8] and Mohamed *et al.*[9] Some of these data were obtained at relatively high pressures and are therefore subject to collisional effects, which were taken into account by extrapolation to zero pressure. We did not utilize these data because the lifetimes have been measured with higher accuracy by other authors cited above and because the pressure-extrapolation introduces additional uncertainties. However, we note that the agreement with Schmoranzer's work[13,15] is usually within 5%, with the exception of the $^4D°_{7/2}$ level, where the results disagree by 37%. We have, therefore, utilized all of the data by Schmoranzer and his colleagues,[13,15] and have applied the data of Bennett *et al.*[5] and Garcia and Campos[6,7] for the remaining 4*p* levels. (No data from Refs. 12, 14, or 21 were available for these.) When the measurements of Garcia and Campos[6,7] are compared with those of Schmoranzer and colleagues,[13,15] one finds differences from −5% to +15% (Garcia and Campos' results are mostly higher). An analogous comparison of the results of Bennett *et al.*[5] and Schmoranzer's group yields differences from −5% to +7%. For this reason and from an analysis of their techniques we attribute to the Bennett *et al.*[5] and the Garcia and Campos[6,7] data uncertainties of ±10% or smaller, which is somewhat larger than their own estimates.

The data of Garcia and Campos[6,7] are very extensive and we utilized their results also for the 4*d* levels (^4D, ^4F). However, the knowledge of lifetimes of 4*d* levels is much less satisfactory than for the 4*p* levels. No high-precision measurement of lifetimes for these levels exists. Furthermore, no lifetimes are measured for the doublet levels 4*d* ^2P and ^2D; and the lifetimes of 4*d* ^2F and ^4P are especially uncertain. This situation is shown in Fig. 2. The results appear to be separated into two distinct groups which differ for some levels by as much as 50%. The data by Blagoev,[35] Zhechev,[36] and Coetzer *et al.*,[37] which have yielded the long lifetimes, have been obtained with techniques prone to cascading effects. Corrections have been carried out by multi-exponential fitting techniques, which are known to be inadequate. However, another similar experiment by Pinnington *et al.*[38] with the same correction technique has provided much shorter lifetimes. These are close to the measurements by Garcia and Campos[7] which are the only ones in which cascading contributions are minimized by electron excitation close to threshold energies.

Owing to the lack of other data for the 4*d* ^4P level, we used the results of an experiment with nonselective electron beam excitation,[35] and assigned it an uncertainty of 30%. As noted before, such experiments have a tendency to produce longer lifetimes and thus smaller A-values.

For deriving additional data from Table 1, we make the assumption that the lifetimes among fine structure levels are identical and thus apply the same results to those fine structure levels for which no measurements have been performed. However, the dependence of lifetimes on fine structure is firmly established only in the cases of the 4*p* ^4D levels. Marger and Schmoranzer[15] found identical results for these levels for different *j*-values, except for the $^4D°_{5/2}$ level, which according to a theoretical analysis by Hibbert and Hansen[33] is due to the special circumstance that this level contains a partial admixture of the $^2D°_{5/2}$ term.

4.2. Emission Experiments

Three types of emission experiments have been applied to the study of Ar II lines: (i) Measurements of "branching ratios" with hollow cathode discharges, i.e. determinations of relative intensities for groups of lines originating from a common upper level; (ii) measurements of relative intensities for lines from different upper levels, which are related through population ratios obtained from equilibrium relations, and (iii) measure-

TABLE 1. Selected lifetime data for Ar II levels

	Atomic level	Lifetime (ns)	Estimated accuracy	References utilized	Comments
$4p$	$^2S^o_{1/2}$	8.7	10%	5,6	Same lifetime has been applied to $j=3/2$ level
	$^2P^o_{1/2}$	8.5	10%	5,6	Also applied to $j=3/2$ level
	$^2P^o_{3/2}$				
	$^2D^o_{5/2}$	9.52	1%	15	Also applied to $j=3/2$ level
	$^4S^o_{3/2}$	7.5	10%	6	Also applied to $j=1/2$, 3/2 levels
	$^4P^o_{5/2}$	7.36	1%	13	
	$^4D^o_{5/2}$	7.54	1%	13	
	$^4D^o_{7/2}$	6.92	1%	13	
$4d$	^2P	–			
	^2D	–			
	$^2F_{7/2}$	3.4	10%	38	Also applied to $j=5/2$ level
	$^4P_{5/2}$	3.9	30%	35	Also applied to $j=1/2$, 3/2 levels
	$^4D_{3/2}$	3.2	10%	7,38	Also applied to $j=1/2$ level
	$^4D_{5/2}$				
	$^4D_{7/2}$				
	$^4F_{5/2}$	3.3	10%	7,38	Also applied to $j=3/2$ level
	$^4F_{7/2}$				
	$^4F_{9/2}$				
$4p'$	$^2P^o_{1/2}$	5.55	10%	6,7	
	$^2P^o_{3/2}$				
	$^2D^o_{5/2}$	8.0	10%	6	Also applied to $j=3/2$ level
	$^2F^o_{5/2}$	8.52	1%	15	
	$^2F^o_{7/2}$	8.41	1%	15	
$4p''$	$^2P^o_{3/2}$	11.0	10%	6	

ments of absolute transition probabilities with wall-stabilized arcs, when local thermodynamic equilibrium (LTE) conditions prevail in these sources.

Hollow cathode discharges are well suited for the determination of branching ratios: the spectrum of ionized species is more readily excited than with a thermal source; because of the low source densities, spectral lines have narrow widths, and possibilities for the blending of lines or misidentifications are greatly reduced; profiles are of the Gaussian type without extended wings (thus, line wing corrections are not necessary for the line ratio measurements); self-absorption is unlikely for the low densities and can be readily checked and controlled by varying the Ar II excited state density or length of the emitting layer.

All critical factors are satisfied in the experiments of Luedtke and Helbig,[39] Hashiguchi and Hasikuni,[40] and Garcia and Campos.[6,7] In some of this work, radiometric calibration was carried out by using two standards; reduction of the noise was achieved by multiple scanning; profile fittings to standard line shape functions were undertaken; self-absorption was checked by varying the emitting plasma layer or the strength of the discharge current; and uncertainties were assessed carefully in each experiment.

The experiment by Luedtke and Helbig[39] has the highest wavelength resolution and covers all branches from the $4p\,^4P$ and ^4D levels. Hashiguchi and Hasikuni[40] have measured numerous other branches; however, many of their sets from specific upper levels are incomplete. Complete sets of emission branches from several levels were determined by Garcia and Campos.[6,7]

Other observations with hollow cathode discharges by Adams and Whaling[41] and Danzmann and Kock[42] were performed utilizing a Fourier transform spectrometer which enables the simultaneous gathering of data over a very large wavelength interval. These data sets do not include weak lines and even some stronger lines which are covered by the above-mentioned observations with hollow cathode discharges. The radiometric calibrations in these two experiments were carried out by applying the branching ratios of accurately known gf values of iron lines and standard sources for the visible spectrum.

An advanced emission experiment was performed by Shumaker and Popenoe[43] in 1969 with a wall-stabilized arc to obtain absolute transition probabilities of the $4s-4p$ and $3d-4p$ Ar II lines. Arc conditions were selected to obtain a state of LTE and the plasma was observed side-on. An Abel-inversion process was then performed on the emission intensity data. Application of line wing corrections, accurate radiometric calibrations, well-defined plasma layers, excellent stability of the source – with reproducibility of the stronger lines at the one percent level, – control of self-absorption and the completeness of data collected for the two transition arrays give these observations a high quality. In a re-

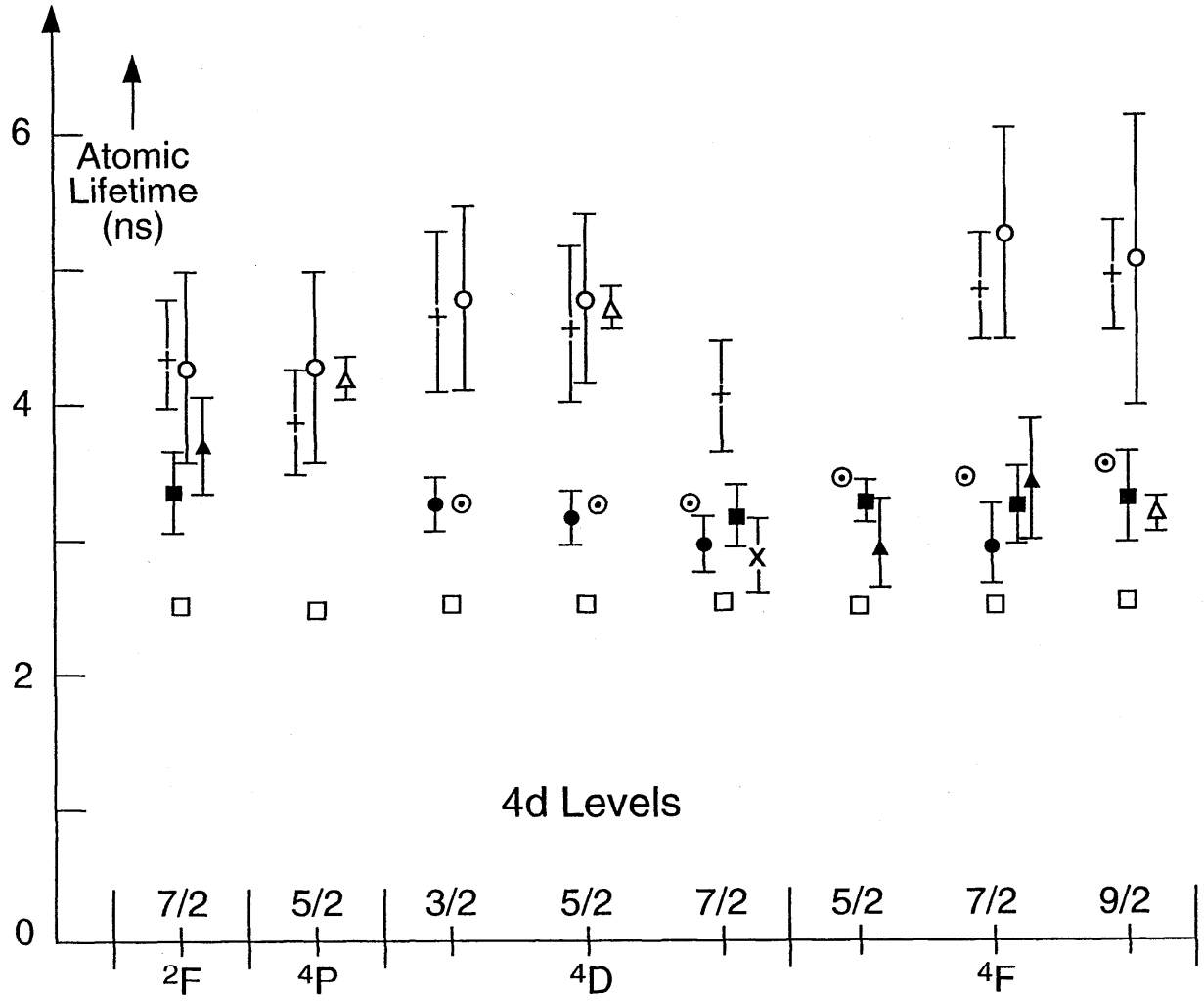

FIG. 2. Lifetime data for 4*d* levels. The symbols denote the following authors:

- ● Garcia and Campos[7] experiment.
- ⊙ Garcia and Campos[7] (theory).
- × Denis and Gaillard[19]
- ▲ Das and Bhattacharaya[25]
- □ Rudko and Tang[29]
- \+ Blagoev[35]
- ○ Zhechev[36]
- △ Coetzer *et al.*[37]
- ■ Pinnington *et al.*[38]

analysis of their data three years later, based on newly available plasma diagnostic material, Shumaker and Popenoe[44] changed their absolute scale by about 10%. This is, however, of no consequence for this study, since we utilize their results only on a relative scale.

Relative transition probabilities were obtained for a limited number of upper levels in a recent study by Dzierzega *et al.*,[45] where a plasma mixture of helium with argon was used to enhance the argon ion spectrum. Several older emission experiments, for example by Schnapauff,[46] by Luyken *et al.*,[47] and by Tidwell[48] were only used for lines where no other data were available, because their data often differ significantly from the work reviewed above.

We found that in all emission experiments of the last 25 years the critical factors listed in Sec. 2 have been clearly addressed and the measurements were carefully done. The applied experimental techniques are quite similar; for example, photoelectric detection has always been used to which automatic data processing has been added in the more recent work. The emission sources are well suited for their purpose: low pressure hollow cathodes for branching ratio determinations, where no state population measurements are required; and higher pressure wall-stabilized arcs which reach LTE conditions so that equilibrium relationships to determine excited state populations for relative and absolute transition probability measurements may be applied.

Thus there are no obvious preferences among the emission data, which is borne out by the comparisons, too. When a set of branches from a specific level is covered by more than one measurement, some data have been found to depart appreciably from the average; these we have excluded. The accuracy of the results is estimated from the following principal sources of error: (i) Uncertainties in the (relative) radiometric calibrations (determination of the spectral sensitivity, or detection efficiency) estimated to be 2% at most, as was borne out by the comparison of two different standards. (ii) reproducibility of line intensities. By monitoring the emission source, the strong lines were usually found to be reproducible to within 1%. Therefore, ratios of line intensities, converted to relative transition probabilities, are for the strong lines in carefully conducted experiments of the order of ±3%, but more typically they are of the order of ±5%. The lines of medium or lower intensity are more difficult to measure, and both the authors' estimates and data comparisons indicate uncertainties for these (which are the majority of lines) of about ±10%, and ±20% or higher for the low intensity lines. Very weak lines are estimated to be uncertain to ±(40–50)%.

4.3. Theory

Until recently, the theoretical approaches to determine transition probabilities of Ar II employed fairly simple atomic structure models, limited to single-configuration approximations. Only Luyken[31] in 1972 used an approach with limited multi-configuration treatment. Hibbert and Hansen[33,34] undertook the first extensive multi-configuration treatment using the computer code CIV3 which produced many significant differences from the earlier theoretical results and the first consistently good agreement with the recent accurate lifetime data. Nevertheless, sometimes significant differences exist between the results of their dipole length and dipole velocity formalisms, even for the strong lines, and they conclude that more accounting of electron correlation is needed. Indeed, the calculated lifetimes (from the preferred dipole-length formalism) lie in all cases somewhat outside the very small error bands of about ±1% obtained for the high-accuracy beam-laser lifetimes by Schmoranzer and colleagues.[13,15] We have therefore not made direct use of any calculated data, but have presented some of the Hibbert and Hansen[33,34] results in a comparison table (Table 2) and in Figs. 1 and 3. These calculations provide excellent independent support to the lifetime-emission data.

TABLE 2. Comparison between theoretical and experimental data: The first data column contains the transition probabilities calculated by Hibbert and Hansen[34] (dipole-length formalism) for those emission lines of the $4s\ ^4P$-$4p\ ^4P^o$ and $3d\ ^4D$-$4p\ ^4P^o$ multiplets which originate from the $4p\ ^4P^o_{5/2}$ level. These are compared with the results derived from the selected branching ratio and lifetime data

Line (nm)	Transition probability ($10^8\ s^{-1}$) Hibbert and Hansen[34]	This compilation
500.93	0.153	0.151 ± 8%
480.60	0.781	0.780 ± 4%
446.06	0.0161	0.015 ± 6%
443.10	0.118	0.109 ± 11%
440.10	0.320	0.304 ± 8%

5. Assembly of the Adopted Data

As discussed above, the set of transition probability data for this tabulation was obtained by combining the most accurate lifetimes available in the literature. Among the lifetime determinations, there are clearly differences in quality and only the best data were utilized. But we found that most branching ratio measurements were of comparable quality, and therefore we applied all of them and averaged the results.

The selected data were then assembled into a set of absolute transition probabilities utilizing the following relationships:

Line intensities I_{ki} for atomic transitions from higher level k to lower level i emitted from a plasma source of length ℓ are related to atomic transition probabilities A_{ki} by

$$I_{ki} = 1/4\pi\ N_k\ h\nu_{ki}\ A_{ki}\ell, \qquad (1)$$

where N_k is the population (per unit volume) and $h\nu_{ki}$ the photon energy. The line intensity is the observed pho-

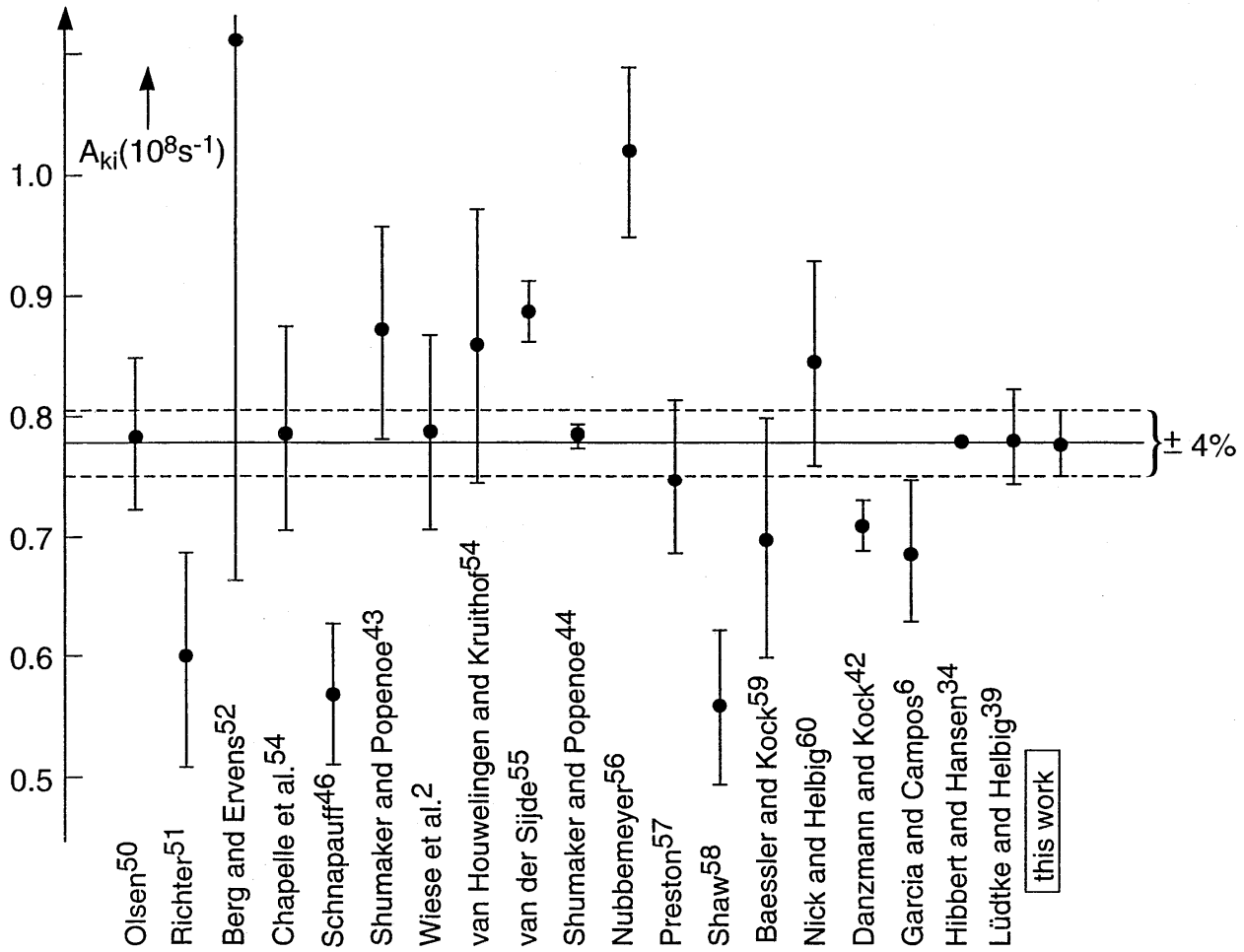

FIG 3. History of transition probability measurements for the 480.6 nm Ar II line over the last 30 years.

toelectric signal S_{ki} divided by the quantum efficiency (or spectral sensitivity) ϵ_{ki} of the spectrometer-detector system at this frequency. In terms of photon intensities $D_{ki} = I_{ki}/h\nu_{ki} = S_{ki}/\epsilon_{ki}h\nu_{ki}$, one obtains from Eq. (1) for the ratio of a pair of lines from upper level k to lower levels m and n

$$L^k_{mn} = D_{km}/D_{kn} = A_{km}/A_{kn} = (S_{km}/S_{kn})\cdot(\epsilon_{kn}/\epsilon_{km})\cdot(h\nu_{kn}/h\nu_{km}) \quad (2)$$

This ratio L, called the branching ratio, is independent of the population of level k and the plasma length ℓ. Also, only relative spectral responses ϵ (i.e., relative radiometric calibrations) are required for such ratios. The transition $k \rightarrow n$ is usually chosen to be a strong line and made a reference transition for a set of lines from level k. The branching fraction R_{km} is

$$R_{km} = A_{km}/\sum_i A_{ki} = L^k_{mn}/\sum_i L^k_{in} \quad (3)$$

where $i = 1,2...,m,n,...$ This branching fraction (which is also often called the branching ratio) provides with the condition $\sum_i R_{ki} = 1$ the connection to the atomic lifetime τ of level k, since τ_k is defined as

$$\tau_k = (\sum_i A_{ki})^{-1}. \quad (4)$$

Therefore,

$$A_{km} = R_{km}/\tau_k = (L^k_{mn}/\sum_i L^k_{in}) \cdot 1/\tau_k \quad (5)$$

We have thus determined absolute transition probabilities A_{ki} from the various published τ_k's and the ratios L^k_{in}. Specific transitions $k \rightarrow n$ have been adopted as arbitrarily chosen reference lines, and ΣL^k_{in} has been normalized to unity in each case. It is very important that these sums are better than 95% complete, that is, complete except for very weak components.

If lines of significant strength from a given upper level are missing, for example, because of being in an inaccessible wavelength range, or blending with lines from

different upper states, we have attempted to supplement the data with other material (see below) or we rejected such a data set.

Additions could be done by using other experimental data or – in a few cases – by using theoretical data. The added intensity reduces, by the same factor, all other contributions within a normalized branching set. The added error depends on the uncertainty of the supplemental line intensities. For example, if the uncertainty is ±30%, as is typical for weak lines, and the added intensity equals 3% of the total, then the error for the other lines of this set increases by only 1%, compared with a 3% systematic error without this addition.

The principal data had to be supplemented with less accurate additions for about half of the branching sets. A few times the semi-empirical calculations of Kurucz and Peytremann[49] were used where we conservatively estimated uncertainties a factor of ±2. However, the additions were always at a level of less than 10%; otherwise, incomplete sets were rejected.

To obtain the branching ratio of one spectral line, the results of different measurements of that line have been averaged and the standard deviation of the mean was evaluated. The error from the addition of missing line intensities was taken into account in the quoted error of the branching ratio by treating it as an independent error. The absolute value of transition probability was then obtained from the averaged branching ratio.

We have taken the branching ratio error as two standard deviations when we had three or more sets of measurements. We rejected experimental data sets which had too little data taken into account, and rejected specific branching ratios when they deviated far from the mean.

The low quality of some experimental approaches became apparent in this way. Because of large scatter, a significant part of the relative transition probabilities from Tidwell[48] (about one-half) and Schnapauff[46] (one third) were rejected.

When only two sets of measurements were available and averaged, the errors of the branching ratio were estimated as 3% for the strongest lines, 8% for the medium strong, and 15% for the weak lines. When only one set was available, the strongest lines were estimated to be uncertain to ±5%, medium lines to ±10%, weak lines to ±20% and very weak lines to ±40% – unless authors specified larger uncertainties.

The error evaluation process clearly shows that the accuracy of the transition probabilities is mainly limited by the branching ratio determinations.

For applications, it is useful to note that from the $4d\ ^4F_{9/2}$ level only one transition (branching ratio equals 1) is allowed. Thus the accuracy with which its lifetime is measured is per definition equal to the accuracy of the relevant transition probability. Somewhat similar are situations in a branching set with a few lines where one of these contains the bulk of the intensity (see e.g. the upper level $4d\ ^2F_{7/2}$).

The overall results of our Ar II data assessment, i.e. listings of recommended transition probabilities ordered according to upper level and according to increasing wavelength, are given in Tables 3 and 4, including our estimated uncertainties.

The result of our analysis for the prominent Ar II line of 480.6 nm is in very close agreement with several recent investigations. A history of all the studies of this particular transition is presented in Fig. 3.[2,6,34,39,42–44,46,50–60] Our result is $0.780 \times 10^8\ s^{-1}$, with a ±4% uncertainty.

Comparisons of the experimentally derived transition probabilities with theory have not shown close agreement until recently. However, the advanced calculations of Hibbert and Hansen[33,34] including detailed electron correlation show a very high degree of agreement with our derived set of data, as seen in Table 2.

Note added in proof: We have just become aware of a new paper by S. A. Young and C. E. Head on "Radiative Lifetime Measurements Using an Argon Ion Beam" in Nucl. Instr. Meth. B56/57, 265 (1991). This is a beam-gas experiment subject to cascading effects, which have been taken into account by a two-exponential decay analysis. This falls according to our grouping of lifetime experiments into the "category (c)" experiments which we have not utilized in our assessment.

TABLE 3. Branching ratios and transition probabilities for Ar II lines ordered according to upper energy level

First line of each set: Upper level	Lifetime plus Uncertainty					
Other lines: Lower level	Wavelength (nm)	Branching ratios	Estimated uncertainty	Transition probability (in 10^8 s^{-1})	Estimated uncertainty
A) Transitions from the 4*p* levels					
$4p\ ^2S^\circ_{1/2}$	8.7 ns ±10%				
$4s\ ^2P_{1/2}$	457.94	0.697	± 2%	0.80	±10%
$^2P_{3/2}$	437.60	0.178	8%	0.205	13%
$^4P_{1/2}$	392.24	0.003	20%	0.003	22%
$^4P_{3/2}$	384.46	<0.003		<0.003	
$3d\ ^2P_{1/2}$	610.35	0.015	30%	0.017	32%
$^2P_{3/2}$	648.31	0.092	11%	0.106	15%
$^2D_{3/2}$	941.86	<0.0034		<0.0039	
$^4P_{3/2}$	735.83	0.001	25%	0.002	27%
$^4F_{3/2}$	564.24	0.001	25%	0.002	27%
$4s'\ ^2D_{3/2}$	801.75	0.007	20%	0.009	22%
$4p\ ^2P^\circ_{1/2}$	8.5 ns ±10%				
$4s\ ^2P_{1/2}$	488.90	0.158	18%	0.19	20%
$^2P_{3/2}$	465.79	0.758	5%	0.89	11%
$^4P_{1/2}$	414.74	<0.002		<0.002	
$^4P_{3/2}$	406.05	<0.001		<0.001	
$3d\ ^2P_{1/2}$	666.64	0.075	4%	0.088	11%
$^2P_{3/2}$	712.17	0.004	20%	0.005	22%
$^4D_{1/2}$	370.69	0.002	20%	0.002	22%
$4p\ ^2P^\circ_{3/2}$	8.5 ns ±10%				
$4s\ ^2P_{1/2}$	476.49	0.545	4%	0.64	11%
$^2P_{3/2}$	454.51	0.400	9%	0.471	14%
$^4P_{1/2}$	405.77	<0.0002		<0.0002	
$^4P_{3/2}$	397.45	0.017	50%	0.020	50%
$^4P_{5/2}$	384.54	0.014	20%	0.016	22%
$3d\ ^2P_{1/2}$	643.76	<0.002		<0.002	
$^4D_{5/2}$	360.15	0.002	20%	0.002	22%
$4p\ ^2D^\circ_{3/2}$	9.52 ns ±1%				
$4s\ ^2P_{1/2}$	496.51	0.375	4%	0.394	4%
$^2P_{3/2}$	472.69	0.556	2%	0.584	3%
$^4P_{1/2}$	420.20	0.020	20%	0.021	20%
$^4P_{3/2}$	411.28	0.010	14%	0.011	14%
$^4P_{5/2}$	397.48	0.009	50%	0.009	50%
$3d\ ^2P_{1/2}$	680.85	0.007	20%	0.007	20%
$^4D_{1/2}$	375.05	0.001	50%	0.001	50%
$^4D_{3/2}$	373.55	0.002	20%	0.003	20%
$^4D_{5/2}$	371.47	0.002	50%	0.002	50%
$^4F_{3/2}$	623.97	0.002	50%	0.002	50%
$^4F_{5/2}$	613.87	0.011	10%	0.012	10%
$4p\ ^2D^\circ_{5/2}$	9.52 ns ±1%				
$4s\ ^2P_{3/2}$	487.99	0.784	2%	0.823	3%
$^4P_{3/2}$	422.82	0.125	3%	0.133	3%
$^4P_{5/2}$	408.24	0.028	7%	0.029	7%
$3d\ ^4D_{3/2}$	383.04	0.004	20%	0.004	20%
$^4D_{5/2}$	380.86	0.010	20%	0.010	20%
$^4D_{7/2}$	378.64	0.014	13%	0.015	13%
$^4F_{3/2}$	650.91	<0.0001		<0.0001	
$^4F_{5/2}$	639.92	0.006	20%	0.006	20%
$^4F_{7/2}$	624.31	0.029	10%	0.030	10%

TABLE 3. Branching ratios and transition probabilities for Ar II lines ordered according to upper energy level – Continued

First line of each set: Upper level		Lifetime plus Uncertainty				
Other lines:						
	Lower level	Wavelength (nm)	Branching ratios	Estimated uncertainty	Transition probability (in 10^8 s^{-1})	Estimated uncertainty
$4p$ $^4S^o_{3/2}$		7.5 ns ±10%				
$4s$	$^2P_{1/2}$	458.79	0.002	25%	0.003	27%
	$^2P_{3/2}$	438.38	0.008	7%	0.011	13%
	$^4P_{1/2}$	392.86	0.183	8%	0.244	13%
	$^4P_{3/2}$	385.06	0.290	6%	0.387	12%
	$^4P_{5/2}$	372.93	0.360	2%	0.480	10%
$3d$	$^2P_{1/2}$	611.87	<0.001		<0.001	
	$^2P_{3/2}$	650.02	0.002	15%	0.003	18%
	$^4P_{1/2}$	723.35	0.028	15%	0.037	18%
	$^4P_{3/2}$	738.04	0.042	15%	0.056	18%
	$^4P_{5/2}$	758.93	0.080	10%	0.107	14%
	$^4D_{3/2}$	351.79	<0.0005		<0.0007	
	$^4D_{5/2}$	349.95	0.002	15%	0.003	18%
$4p$ $^4P^o_{1/2}$		7.36 ns ±1%				
$4s$	$^2P_{1/2}$	607.74	0.003	20%	0.004	20%
	$^2P_{3/2}$	572.43	0.003	20%	0.004	20%
	$^4P_{1/2}$	497.22	0.072	7%	0.097	7%
	$^4P_{3/2}$	484.78	0.625	9%	0.849	9%
$3d$	$^4D_{1/2}$	435.22	0.156	9%	0.212	9%
	$^4D_{3/2}$	433.20	0.141	6%	0.192	6%
$4p$ $^4P^o_{3/2}$		7.36 ns ±1%				
$4s$	$^2P_{1/2}$	621.22	<0.0005		<0.0007	
	$^2P_{3/2}$	584.38	<0.0003		<0.0004	
	$^4P_{1/2}$	506.20	0.164	11%	0.223	11%
	$^4P_{3/2}$	493.32	0.106	5%	0.144	5%
	$^4P_{5/2}$	473.59	0.427	2%	0.580	3%
$3d$	$^4D_{1/2}$	442.09	0.023	11%	0.031	11%
	$^4D_{3/2}$	440.01	0.118	11%	0.160	11%
	$^4D_{5/2}$	437.13	0.162	8%	0.221	8%
$4p$ $^4P^o_{5/2}$		7.36 ns ±1%				
$4s$	$^2P_{3/2}$	595.09	<0.0005		<0.0007	
	$^4P_{3/2}$	500.93	0.111	8%	0.151	8%
	$^4P_{5/2}$	480.60	0.574	3%	0.780	4%
$3d$	$^4D_{3/2}$	446.06	0.011	6%	0.015	6%
	$^4D_{5/2}$	443.10	0.080	11%	0.109	11%
	$^4D_{7/2}$	440.10	0.224	8%	0.304	8%
$4p$ $^4D^o_{1/2}$		6.92 ns ±1%				
$4s$	$^2P_{1/2}$	521.51	<0.0009		<0.0013	
	$^2P_{3/2}$	495.29	0.004	50%	0.006	50%
	$^4P_{1/2}$	437.97	0.695	3%	1.004	4%
	$^4P_{3/2}$	428.29	0.090	9%	0.132	9%
$3d$	$^4P_{1/2}$	892.61	0.004	20%	0.006	20%
	$^4P_{3/2}$	915.08	<0.0035		<0.0045	
	$^4D_{1/2}$	389.14	0.030	15%	0.043	15%
	$^4D_{3/2}$	387.53	0.057	14%	0.082	14%
	$^4F_{3/2}$	663.97	0.117	5%	0.169	5%

TABLE 3. Branching ratios and transition probabilities for Ar II lines ordered according to upper energy level – Continued

First line of each set: Upper level	Lifetime plus Uncertainty					
Other lines: Lower level	Wavelength (nm)	Branching ratios	Estimated uncertainty	Transition probability (in 10^8 s^{-1})	Estimated uncertainty	
$4p\ ^4D^\circ_{3/2}$	6.92 ns ±1%					
$4s\ ^2P_{1/2}$	528.69	0.002	30%	0.002	30%	
$^2P_{3/2}$	501.76	0.007	15%	0.011	15%	
$^4P_{1/2}$	443.02	0.394	4%	0.569	4%	
$^4P_{3/2}$	433.12	0.397	5%	0.574	5%	
$^4P_{5/2}$	417.84	0.008	18%	0.012	18%	
$3d\ ^4D_{1/2}$	393.12	0.014	9%	0.020	9%	
$^4D_{3/2}$	391.48	0.026	11%	0.037	11%	
$^4D_{5/2}$	389.20	0.044	23%	0.063	23%	
$^4F_{3/2}$	675.66	0.014	15%	0.020	15%	
$^4F_{5/2}$	663.82	0.095	5%	0.137	5%	
$4p\ ^4D^\circ_{5/2}$	7.54 ns ±1%					
$4s\ ^2P_{3/2}$	514.53	0.080	9%	0.106	9%	
$^4P_{3/2}$	442.60	0.616	5%	0.817	5%	
$^4P_{5/2}$	426.65	0.124	11%	0.164	11%	
$3d\ ^4D_{3/2}$	399.21	0.012	15%	0.016	15%	
$^4D_{5/2}$	396.84	0.036	9%	0.048	9%	
$^4D_{7/2}$	394.43	0.031	14%	0.041	14%	
$^4F_{3/2}$	699.01	0.001	20%	0.002	20%	
$^4F_{5/2}$	686.35	0.019	10%	0.025	10%	
$^4F_{7/2}$	668.43	0.081	8%	0.107	8%	
$4p\ ^4D^\circ_{7/2}$	6.92 ns ±1%					
$4s\ ^4P_{5/2}$	434.81	0.810	4%	1.171	4%	
$3d\ ^4D_{5/2}$	403.88	0.008	10%	0.012	10%	
$^4D_{7/2}$	401.39	0.073	5%	0.105	5%	
$^4F_{5/2}$	707.70	0.001	20%	0.001	20%	
$^4F_{7/2}$	686.66	0.006	10%	0.009	10%	
$^4F_{9/2}$	664.37	0.102	10%	0.147	10%	

B) Transitions from the 4*d* levels

$4d\ ^2P_{1/2}$	Lifetime not measured					
$4d\ ^2P_{3/2}$	Lifetime not measured					
$4d\ ^2D_{3/2}$	Lifetime and branching ratios not measured					
$4d\ ^2D_{5/2}$	Lifetime not measured					
$4d\ ^2F_{5/2}$	4.4 ns ±30%	Branching ratios poorly measured				
$4d\ ^2F_{7/2}$	3.4 ns ±10%					
$4p\ ^2D^\circ_{5/2}$	355.95	0.978	3%	2.88	10%	
$^4P^\circ_{5/2}$	314.64	0.001	20%	0.003	22%	
$^4D^\circ_{5/2}$	343.04	0.021	10%	0.062	14%	
$4d\ ^4P_{1/2}$	3.9 ns ±30%					
$4p\ ^2P^\circ_{1/2}$	377.75	0.004	15%	0.011	35%	
$^4S^\circ_{3/2}$	397.94	0.384	6%	0.98	31%	
$^4P^\circ_{1/2}$	328.17	0.164	6%	0.42	31%	
$^4P^\circ_{3/2}$	324.37	0.412	6%	1.1	31%	

TABLE 3. Branching ratios and transition probabilities for Ar II lines ordered according to upper energy level – Continued

First line of each set: Upper level		Lifetime plus Uncertainty				
Other lines:						
	Lower level	Wavelength (nm)	Branching ratios	Estimated uncertainty	Transition probability (in 10^8 s^{-1})	Estimated uncertainty
$4d$ $^4P_{3/2}$		3.9 ns ±30%				
$4p$	$^4S°_{3/2}$	393.25	0.363	9%	0.93	31%
	$^4P°_{1/2}$	324.98	0.246	9%	0.63	31%
	$^4P°_{3/2}$	321.25	0.020	10%	0.052	32%
	$^4P°_{5/2}$	318.10	0.144	5%	0.37	30%
	$^4D°_{1/2}$	356.50	0.215	5%	0.56	30%
$4d$ $^4P_{5/2}$		3.9 ns ±30%				
$4p$	$^2D°_{5/2}$	355.00	0.010	10%	0.026	32%
	$^4S°_{3/2}$	386.85	0.528	8%	1.4	31%
	$^4P°_{3/2}$	316.97	0.192	10%	0.49	32%
	$^4P°_{5/2}$	313.90	0.203	7%	0.52	31%
$4d$ $^4D_{1/2}$		3.2 ns ±10%				
$4p$	$^2D°_{3/2}$	403.14	0.024	10%	0.075	14%
	$^4P°_{1/2}$	350.98	0.815	5%	2.55	11%
	$^4D°_{1/2}$	388.03	0.074	10%	0.233	14%
	$^4D°_{3/2}$	384.15	0.086	10%	0.269	14%
$4d$ $^4D_{3/2}$		3.2 ns ±10%				
$4p$	$^2P°_{3/2}$	420.99	0.0006	50%	0.0018	50%
	$^2D°_{3/2}$	406.51	0.003	20%	0.011	22%
	$^2D°_{5/2}$	395.84	0.012	10%	0.038	14%
	$^4S°_{3/2}$	435.85	<0.0006		<0.0018	
	$^4P°_{1/2}$	353.53	0.181	10%	0.57	14%
	$^4P°_{3/2}$	349.12	0.574	5%	1.79	11%
	$^4P°_{5/2}$	345.41	0.100	11%	0.314	15%
	$^4D°_{1/2}$	391.16	0.025	14%	0.077	17%
	$^4D°_{3/2}$	387.21	0.049	18%	0.15	20%
	$^4D°_{5/2}$	379.94	0.055	20%	0.17	22%
$4d$ $^4D_{5/2}$		3.2 ns ±10%				
$4p$	$^2P°_{3/2}$	424.36	0.001	20%	0.002	22%
	$^2D°_{5/2}$	398.82	0.013	7%	0.041	13%
	$^4S°_{3/2}$	439.46	0.002	20%	0.006	22%
	$^4P°_{3/2}$	351.44	0.425	4%	1.36	11%
	$^4P°_{5/2}$	347.67	0.389	3%	1.25	11%
	$^4D°_{3/2}$	390.06	0.023	5%	0.072	11%
	$^4D°_{5/2}$	382.68	0.090	5%	0.281	11%
	$^4D°_{7/2}$	376.35	0.057	5%	0.178	11%
$4d$ $^4D_{7/2}$		3.2 ns ±10%				
$4p$	$^4P°_{5/2}$	349.15	0.739	1%	2.31	11%
	$^4D°_{5/2}$	384.47	0.016	15%	0.048	15%
	$^4D°_{7/2}$	378.08	0.245	1%	0.77	11%
$4d$ $^4F_{3/2}$		3.15 ns ±10%				
$4p$	$^2D°_{3/2}$	370.99	0.015	11%	0.047	15%
	$^4S°_{3/2}$	395.27	0.066	11%	0.208	15%
	$^4P°_{1/2}$	326.36	0.049	11%	0.155	15%
	$^4P°_{3/2}$	322.60	0.007	20%	0.021	22%
	$^4D°_{1/2}$	358.16	0.555	6%	1.76	12%
	$^4D°_{3/2}$	354.85	0.275	6%	0.87	12%

TABLE 3. Branching ratios and transition probabilities for Ar II lines ordered according to upper energy level — Continued

First line of each set: Upper level	Lower level	Wavelength (nm)	Branching ratios	Estimated uncertainty	Transition probability (in 10^8 s^{-1})	Estimated uncertainty
Other lines:						
$4d\ ^4F_{5/2}$		3.30 ns ±10%				
$4p$	$^2P^\circ_{3/2}$	386.96	0.002	20%	0.006	22%
	$^2D^\circ_{3/2}$	374.69	0.007	10%	0.021	14%
	$^2D^\circ_{5/2}$	365.60	0.025	9%	0.076	14%
	$^4P^\circ_{3/2}$	325.39	0.003	20%	0.009	22%
	$^4P^\circ_{5/2}$	322.16	0.006	22%	0.018	24%
	$^4D^\circ_{3/2}$	358.24	0.776	3%	2.35	11%
	$^4D^\circ_{5/2}$	352.00	0.174	3%	0.52	11%
	$^4D^\circ_{7/2}$	346.63	0.010	15%	0.030	18%
$4d\ ^4F_{7/2}$		3.30 ns ±10%				
$4p$	$^2D^\circ_{5/2}$	371.72	0.017	7%	0.052	13%
	$^4D^\circ_{5/2}$	357.66	0.908	1%	2.75	10%
	$^4D^\circ_{7/2}$	352.13	0.075	3%	0.227	11%
$4d\ ^4F_{9/2}$		3.30 ns ±10%				
$4p$	$^4D^\circ_{7/2}$	358.84	1.000	0% (per def.)	3.03	10%
C) Transitions from the $4p'$ and $4p''$ levels						
$4p''\ ^2P^\circ_{1/2}$		5.55 ns ±10%				
$3d$	$^2P_{1/2}$	355.69	0.028	10%	0.050	14%
	$^2P_{3/2}$	368.25	0.010	10%	0.017	14%
	$^2D_{3/2}$	447.48	0.161	5%	0.290	11%
$4s$	$^2P_{1/2}$	297.91	0.231	3%	0.416	11%
	$^2P_{3/2}$	289.16	0.101	4%	0.182	11%
$4s'$	$^2D_{3/2}$	413.17	0.469	4%	0.85	11%
$4p'\ ^2P^\circ_{3/2}$		5.55 ns ±10%				
$3d$	$^2P_{1/2}$	363.48	0.005	20%	0.009	22%
	$^2P_{3/2}$	376.61	0.041	10%	0.074	14%
	$^2D_{3/2}$	459.88	0.037	3%	0.067	11%
	$^2D_{5/2}$	473.21	0.037	10%	0.067	14%
	$^2F_{5/2}$	453.05	0.012	5%	0.021	11%
	$^4P_{1/2}$	400.11	0.003	20%	0.006	22%
	$^4P_{3/2}$	404.57	0.009	25%	0.016	27%
$4s$	$^2P_{1/2}$	303.35	0.055	3%	0.099	11%
	$^2P_{3/2}$	294.29	0.293	3%	0.53	11%
	$^4P_{3/2}$	269.26	0.003	20%	0.005	22%
$4s'$	$^2D_{3/2}$	423.72	0.062	3%	0.112	11%
	$^2D_{5/2}$	427.75	0.443	3%	0.80	11%
$4p'\ ^2D^\circ_{3/2}$		8.0 ns ±10%				
$3d$	$^2P_{3/2}$	361.18	0.005	20%	0.006	22%
	$^2D_{3/2}$	437.08	0.530	5%	0.66	11%
	$^2D_{5/2}$	449.10	0.037	8%	0.046	13%
$4s$	$^2P_{1/2}$	293.26	0.006	20%	0.008	22%
	$^2P_{3/2}$	284.78	0.002	20%	0.003	22%
$4s'$	$^2D_{3/2}$	404.29	0.325	8%	0.406	13%
	$^2D_{5/2}$	407.96	0.095	8%	0.119	13%

TABLE 3. Branching ratios and transition probabilities for Ar II lines ordered according to upper energy level – Continued

First line of each set: Upper level		Lifetime plus Uncertainty				
Other lines:						
	Lower level	Wavelength (nm)	Branching ratios	Estimated uncertainty	Transition probability (in 10^8 s^{-1})	Estimated uncertainty
$4p'\ ^2D^o_{5/2}$		8.0 ns ±10%				
$3d$	$^2P_{3/2}$	360.59	0.035	10%	0.044	14%
	$^2D_{3/2}$	436.21	0.044	4%	0.055	11%
	$^2D_{5/2}$	448.18	0.364	5%	0.455	11%
	$^2F_{5/2}$	430.06	0.046	9%	0.058	14%
	$^2F_{7/2}$	412.86	0.011	7%	0.014	12%
	$^4P_{5/2}$	391.78	0.001	20%	0.001	22%
$4s$	$^2P_{3/2}$	284.41	0.001	20%	0.002	22%
$4s'$	$^2D_{3/2}$	403.55	0.035	1%	0.044	10%
	$^2D_{5/2}$	407.20	0.463	4%	0.58	11%
$4p'\ ^2F^o_{3/2}$		8.52 ns ±1%				
$3d$	$^2P_{3/2}$	404.22	0.003	20%	0.004	20%
	$^2D_{3/2}$	501.72	0.176	4%	0.207	4%
	$^2D_{5/2}$	517.62	0.015	10%	0.017	10%
	$^2F_{5/2}$	493.61	0.006	20%	0.007	20%
	$^2F_{7/2}$	471.08	0.004	20%	0.005	20%
$3d'$	$^2G_{7/2}$	617.23	0.170	2%	0.200	3%
$4s'$	$^2D_{3/2}$	458.99	0.566	3%	0.664	4%
	$^2D_{5/2}$	463.72	0.060	3%	0.071	3%
$4p'\ ^2F^o_{7/2}$		8.41 ns ±1%				
$4s$	$^4P_{5/2}$	275.49	0.002	20%	0.002	20%
$3d$	$^2D_{5/2}$	514.18	0.068	3%	0.081	4%
	$^2F_{5/2}$	490.48	0.031	7%	0.037	7%
	$^2F_{7/2}$	468.23	0.007	20%	0.008	20%
	$^4P_{5/2}$	441.29	0.051	10%	0.061	10%
$3d'$	$^2G_{7/2}$	612.34	0.008	20%	0.009	20%
	$^2G_{9/2}$	611.49	0.168	6%	0.200	6%
$4s'$	$^2D_{5/2}$	460.96	0.665	3%	0.789	4%
$4p'\ ^2P^o_{3/2}$		11.0 ns ±10%				
$4s'$	$^2D_{5/2}$	231.77	0.151	20%	0.14	22%
$4s'$	$^2S_{1/2}$	405.29	0.735	20%	0.67	22%

TABLE 4. Recommended transition probabilities of Ar II lines arranged according to wavelength

Wavelength (nm)	Upper energy level E_k (cm^{-1})	Statistical weight g_i	Statistical weight g_k	Transition probability (in 10^8 s^{-1})	Estimated uncertainty (in %)
231.77	191975	6	4	0.14	22
269.26	172214	4	4	0.005	22
275.49	170530	6	8	0.002	20
284.41	173393	4	6	0.002	22
284.78	173348	4	4	0.003	22
289.16	172816	4	2	0.182	11
293.26	173348	2	4	0.008	22
294.29	172214	4	4	0.53	11
297.91	172816	2	2	0.416	11
303.35	172214	2	4	0.099	11
313.90	186891	6	6	0.52	31
314.64	186816	6	8	0.003	41
316.97	186891	4	6	0.49	32
318.10	186470	6	4	0.37	30
321.25	186470	4	4	0.052	32
322.16	186074	6	6	0.018	24
322.60	186341	4	4	0.021	22
324.37	186171	4	2	1.056	31
324.98	186470	2	4	0.63	31
325.39	186074	4	6	0.009	22
326.36	186341	2	4	0.155	15
328.17	186171	2	2	0.42	31
343.04	186816	6	8	0.062	14
345.41	183986	6	4	0.314	15
346.63	186074	8	6	0.030	18
347.67	183797	6	6	1.25	11
349.12	183986	4	4	1.79	11
349.15	183676	6	8	2.31	11
349.95	161049	6	4	0.003	18
350.98	184192	2	2	2.55	11
351.44	183797	4	6	1.36	11
351.79	161049	4	4	<0.0007	
352.00	186074	6	6	0.52	11
352.13	185625	8	8	0.227	11
353.53	183986	2	4	0.57	14
354.85	186341	4	4	0.87	12
355.00	186891	6	6	0.026	32
355.69	172816	2	2	0.050	14
355.95	186816	6	8	2.88	10
356.50	186470	2	4	0.55	30
357.66	185625	6	8	2.75	10
358.16	186341	2	4	1.76	12
358.24	186074	4	6	2.53	11
358.84	185093	8	10	3.03	10
360.15	160239	6	4	0.002	22
360.59	173393	4	6	0.044	14
361.18	173348	4	4	0.006	22
363.48	172214	2	4	0.009	22
365.60	186074	6	6	0.076	14
368.25	172816	4	2	0.017	14
370.69	159707	2	2	0.002	22
370.99	186341	4	4	0.047	15
371.47	159393	6	4	0.002	50
371.72	185625	6	8	0.052	13
372.93	161049	6	4	0.480	10
373.55	159393	4	4	0.003	20
374.69	186074	4	6	0.021	14
375.05	159393	2	4	0.001	50
376.35	183797	8	6	0.178	11
376.61	172214	4	4	0.074	14
377.75	186171	2	2	0.011	35
378.08	183676	8	8	0.77	11
378.64	158730	8	6	0.015	13
379.94	183986	6	4	0.17	22

TABLE 4. Recommended transition probabilities of Ar II lines arranged according to wavelength – Continued

Wavelength (nm)	Upper energy level E_k (cm^{-1})	Statistical weight g_i	Statistical weight g_k	Transition probability (in 10^8 s^{-1})	Estimated uncertainty (in %)
380.86	158730	6	6	0.010	20
382.68	183797	6	6	0.281	11
383.04	158730	4	6	0.004	20
384.15	184192	4	2	0.269	14
384.46	161089	4	2	<0.003	
384.47	183676	6	8	0.048	15
384.54	160239	6	4	0.016	22
385.06	161049	4	4	0.387	12
386.85	186891	4	6	1.4	31
386.96	186074	4	6	0.006	22
387.21	183986	4	4	0.15	20
387.53	158428	4	2	0.082	14
388.03	184192	2	2	0.232	14
389.14	158428	2	2	0.043	15
389.20	158168	6	4	0.063	23
390.06	183797	4	6	0.072	11
391.16	183986	2	4	0.077	17
391.48	158168	4	4	0.037	11
391.78	173393	6	6	0.001	22
392.24	161089	2	2	0.003	22
392.86	161049	2	4	0.244	13
393.12	158168	2	4	0.020	9
393.25	186470	4	4	0.93	31
394.43	157673	8	6	0.041	14
395.27	186341	4	4	0.208	15
395.84	183986	6	4	0.038	14
396.84	157673	6	6	0.048	9
397.45	160239	4	4	0.020	50
397.48	159393	6	4	0.009	50
397.94	186171	4	2	0.98	31
398.82	183797	6	6	0.041	13
399.21	157673	4	6	0.016	15
400.11	172214	2	4	0.006	22
401.39	157234	8	8	0.105	5
403.14	184192	4	2	0.075	14
403.55	173393	4	6	0.044	10
403.88	157234	6	8	0.012	10
404.22	170401	4	6	0.004	20
404.29	173348	4	4	0.406	13
404.57	172214	4	4	0.016	27
405.29	191975	2	4	0.67	22
405.77	160239	2	4	<0.000	2
406.05	159707	4	2	<0.001	
406.51	183986	4	4	0.011	22
407.20	173393	6	6	0.58	11
407.96	173348	6	4	0.119	13
408.24	158730	6	6	0.029	7
411.28	159393	4	4	0.011	14
412.86	173393	8	6	0.014	12
413.17	172816	4	2	0.85	11
414.74	159707	2	2	<0.002	
417.84	158168	6	4	0.012	18
420.20	159393	2	4	0.021	20
420.99	183986	4	4	0.0018	50
422.82	158730	4	6	0.131	3
423.72	172214	4	4	0.112	11
424.36	183797	4	6	0.002	22
426.65	157673	6	6	0.164	11
427.75	172214	6	4	0.80	11
428.29	158428	4	2	0.132	9
430.06	173393	6	6	0.057	14
433.12	158168	4	4	0.574	5
433.20	155708	4	2	0.192	6
434.81	157234	6	8	1.171	4

TABLE 4. Recommended transition probabilities of Ar II lines arranged according to wavelength – Continued

Wavelength (nm)	Upper energy level E_k (cm^{-1})	Statistical weight g_i	Statistical weight g_k	Transition probability (in 10^8 s^{-1})	Estimated uncertainty (in %)
435.22	155708	2	2	0.212	9
435.85	183986	4	4	<0.0018	
436.21	173393	4	6	0.055	11
437.08	173348	4	4	0.66	11
437.13	155351	6	4	0.221	8
437.60	161089	4	2	0.205	13
437.97	158428	2	2	1.004	4
438.38	161049	4	4	0.011	13
439.46	183797	4	6	0.006	22
440.01	155351	4	4	0.160	11
440.10	155043	8	6	0.304	8
441.29	170530	6	8	0.061	10
442.09	155351	2	4	0.031	11
442.60	157673	4	6	0.817	5
443.02	158168	2	4	0.569	4
443.10	155043	6	6	0.109	11
446.06	155043	4	6	0.015	6
447.48	172816	4	2	0.290	11
448.18	173393	6	6	0.455	11
449.10	173348	6	4	0.046	13
453.05	172214	6	4	0.021	11
454.51	160239	4	4	0.471	14
457.94	161089	2	2	0.80	10
458.79	161049	2	4	0.003	27
458.99	170401	4	6	0.664	4
459.88	172214	4	4	0.067	11
460.96	170530	6	8	0.789	4
463.72	170401	6	6	0.071	3
465.79	159707	4	2	0.892	11
468.23	170530	8	8	0.008	20
471.08	170401	8	6	0.005	20
472.69	159393	4	4	0.588	3
473.21	172214	6	4	0.067	14
473.59	155351	6	4	0.580	3
476.49	160239	2	4	0.64	11
480.60	155043	6	6	0.780	4
484.78	155708	4	2	0.849	9
487.99	158730	4	6	0.823	3
488.90	159707	2	2	0.19	20
490.48	170530	6	8	0.037	7
493.32	155351	4	4	0.144	5
493.61	170401	6	6	0.007	20
495.29	158428	4	2	0.006	50
496.51	159393	2	4	0.394	4
497.22	155708	2	2	0.097	7
500.93	155043	4	6	0.151	8
501.72	170401	4	6	0.207	4
501.76	158168	4	4	0.011	15
506.20	155351	2	4	0.223	11
514.18	170530	6	8	0.081	4
514.53	157673	4	6	0.106	9
517.62	170401	6	6	0.017	10
521.51	158428	2	2	<0.0013	
528.69	158168	2	4	0.002	30
564.24	161089	4	2	0.002	27
572.43	155708	4	2	0.004	20
584.38	155351	4	4	<0.0004	
595.09	155043	4	6	<0.0007	
607.74	155708	2	2	0.004	20
610.35	161089	2	2	0.017	32
611.49	170530	10	8	0.200	6
611.87	161049	2	4	<0.001	
612.34	170530	8	8	0.009	20
613.87	159393	6	4	0.012	10

TABLE 4. Recommended transition probabilities of Ar II lines arranged according to wavelength – Continued

Wavelength (nm)	Upper energy level E_k(cm^{-1})	Statistical weight g_i	Statistical weight g_k	Transition probability (in 10^8 s^{-1})	Estimated uncertainty (in %)
617.23	170401	8	6	0.200	3
621.22	155351	2	4	<0.0007	
623.97	159393	4	4	0.002	50
624.31	158730	8	6	0.030	10
639.92	158730	6	6	0.006	20
643.76	160239	2	4	<0.002	
648.31	161089	4	2	0.106	15
650.02	161049	4	4	0.003	18
650.91	158730	4	6	<0.0001	
663.82	158168	6	4	0.137	5
663.97	158428	4	2	0.169	5
664.37	157234	10	8	0.147	10
666.64	159707	2	2	0.088	11
668.43	157673	8	6	0.107	8
675.66	158168	4	4	0.020	15
680.85	159393	2	4	0.007	20
686.35	157673	6	6	0.025	10
686.66	157234	8	8	0.009	20
699.01	157673	4	6	0.002	20
707.70	157234	6	8	0.001	22
712.17	159707	4	2	0.005	18
723.35	161049	2	4	0.037	27
735.83	161089	4	2	0.002	18
738.04	161049	4	4	0.056	14
758.93	161049	6	4	0.107	22
801.75	161089	4	2	0.009	22
892.61	158428	2	2	0.006	20
915.08	158428	4	2	<0.0045	
941.86	161089	4	2	<0.0039	

6. Acknowledgement

One of us (V. V.) gratefully acknowledges the partial support of the U.S.-Yugoslavian Joint Fund for Scientific and Technological Cooperation.

7. References

[1]W. L. Wiese, J. W. Brault, K. Danzmann, V. Helbig, and M. Kock, Phys. Rev. A **39**, 2461 (1989).
[2]W. L. Wiese, M. W. Smith, and B. M. Miles, "Atomic Transition Probabilities-Sodium through Calcium," NSRDS-NBS 22, U. S. Gov't. Print. Off., Washington, D. C. (1969).
[3]G. Norlén, Phys. Scr. **8**, 249 (1973).
[4]A. R. Striganov and G. A. Odintsova, "Tables of Spectral Lines of Atoms and Ions," Energoizdat, Moscow (1982).
[5]W. R. Bennett, P. J. Kindlmann, G. N. Mercer, and J. Sunderland, Appl. Phys. Lett. **5**, 158 (1964).
[6]G. Garcia and J. Campos, J. Quant. Spectrosc. Radiat. Transfer **34**, 85 (1985).
[7]G. Garcia and J. Campos, Phys. Scr. **33**, 321 (1986).
[8]C. Camhy-Val, A. M. Dumont, M. Dreux, L. Perret, and C. Vanderriest, J. Quant. Spectrosc. Radiat. Transfer **15**, 527 (1975).
[9]K. A. Mohamed, G. C. King, and F. H. Read, J. Phys. **B 9**, 3159 (1976).
[10]W. L. Wiese, Nucl. Instrum. Methods **90**, 25 (1970).
[11]L. C. Curtis, in "Beam-Foil Spectroscopy," Chapter 3, Ed. S. Bashkin, Springer-Verlag, Berlin (1976).
[12]L. Ward, A. Wännström, A. Arnesen, R. Hallin, and O. Vogel, Phys. Scr. **31**, 149 (1985).
[13]H. Schmoranzer, P. Hartmetz, and D. Marger, J. Phys. **B 19**, 1023 (1986).
[14]W. Schade, Z. Stryla, V. Helbig, and G. Langhans, Phys. Scr. **39**, 246 (1989).
[15]D. Marger and H. Schmoranzer, Phys. Lett. **150A**, 196 (1990).
[16]T. Breuning, M. Elbel, and R. Quad, Ann. Phys. (Paris) **7**, 103 (1985).
[17]U. Fink, S. Bashkin, and W. S. Bickel, J. Quant. Spectrosc. Radiat. Transfer **10**, 1241 (1970).
[18]G. E. Assousa, L. Brown, and W. K. Ford, Jr., J. Opt. Soc. Am. **60**, 1311 (1970).
[19]A. Denis and M. Gaillard, Phys. Lett. **31A**, 9 (1970).
[20]T. Andersen, O. H. Madsen, and G. Sorensen, Phys. Scr. **6**, 125 (1972).
[21]F. J. Coetzer, T. C. Kotze, and P. van der Westhuizen, J. Quant. Spectrosc. Radiat. Transfer **38**, 253 (1987).
[22]D. B. King and C. E. Head, Phys. Rev. A **13**, 1778 (1976).
[23]J. Bakos, J. Szigeti, and L. Varga, Phys. Lett. **20**, 503 (1966).
[24]M. B. Das and R. Bhattacharaya, Z. Phys. **D 14**, 25 (1989).
[25]M. B. Das and R. Bhattacharaya, J. Phys. **B 24**, 423 (1991).
[26]M. L. Burshtein, private communication.
[27]R. H. Garstang, Mon. Not. R. Astron. Soc. **114**, 118 (1954).
[28]H. Statz, F. A. Horrigan, S. H. Koozekanani, C. L. Tang, and G. F. Koster, J. Appl. Phys. **36**, 2278 (1965).
[29]R. I. Rudko and C. L. Tang, J. Appl. Phys. **38**, 4731 (1967).
[30]S. H. Koozekanani and G. L. Trusty, J. Opt. Soc. Am. **59**, 1281 (1969).
[31]B. F. J. Luyken, Physica **60**, 432 (1972).
[32]A. V. Loginov and P. F. Gruzdev, Opt. Spectrosc. (USSR) **44**, 500 (1978).
[33]A. Hibbert and J. E. Hansen, Nucl. Instrum. Methods **B31**, 273 (1988).
[34]A. Hibbert and J. E. Hansen, J. Phys. **B 22**, L347 (1989).
[35]K. B. Blagoev, J. Phys. **B 16**, 33 (1983).

[36]D. Zhechev, J. Phys. **B 18**, 65 (1985).
[37]F. J. Coetzer, T. C. Kotze, and P. van der Westhuizen, J. Quant. Spectrosc. Radiat. Transfer **39**, 181 (1988).
[38]E. H. Pinnington, P. Weinberg, W. Verfuss, H. D. Lutz, and R. Hippler, Phys. Lett. **65A**, 287 (1978).
[39]T. Luedtke and V. Helbig, J. Quant. Spectrosc. Radiat. Transfer **44**, 261 (1990).
[40]S. Hashiguchi and M. Hasikuni, J. Phys. Soc. Japan **54**, 1290 (1985).
[41]D. L. Adams and W. Whaling, J. Opt. Soc. Am. **71**, 1036 (1981).
[42]K. Danzmann and M. Kock, J. Quant. Spectrosc. Radiat. Transfer **29**, 517 (1983).
[43]J. B. Shumaker and C. H. Popenoe, J. Opt. Soc. Am. **59**, 980 (1969).
[44]J. B. Shumaker and C. H. Popenoe, J. Res. Nat. Bur. Stand., Sect. A **76**, 71 (1972).
[45]K. Dzierzega, M. Kubala, S. Labuz, K. Musiol, and B. Pokrzywka, Acta Phys. Pol. A **78**, 299 (1990).
[46]R. Schnapauff, Z. Astrophys. **68**, 431 (1968).
[47]B. F. J. Luyken, F. J. De Heer, R. Ch. Baas, and H. Tawara, Physica **62**, 249 (1972).
[48]E. D. Tidwell, J. Quant. Spectrosc. Radiat. Transfer **12**, 431 (1972).
[49]R. E. Kurucz and E. Peytremann, S. A. O. Spec. Rep. No. 362, (1975).
[50]H. N. Olsen, J. Quant. Spectrosc. Radiat. Transfer **3**, 305 (1963).
[51]J. Richter, Z. Astrophys. **61**, 57 (1965).
[52]H. F. Berg and W. Ervens, Z. Phys. **206**, 184 (1967).
[53]J. Chapelle, A. Sy, F. Cabannes, and J. Blandin, J. Quant. Spectrosc. Radiat. Transfer **8**, 1201 (1968).
[54]D. van Houwelingen and A. A. Kruithof, J. Quant. Spectrosc. Radiat. Transfer **11**, 1235 (1971).
[55]B. van der Sijde, J. Quant. Spectrosc. Radiat. Transfer **12**, 703 (1972).
[56]H. Nubbemeyer, J. Quant. Spectrosc. Radiat. Transfer **16**, 395 (1976).
[57]R. C. Preston, J. Phys. **B 10**, 1377 (1977).
[58]C. B. Shaw, Jr. J. Quant. Spectrosc. Radiat. Transfer **24**, 259 (1980).
[59]P. Baessler and M. Kock, J. Phys. **B 13**, 1351 (1980).
[60]K. -P. Nick and V. Helbig, J. Quant. Spectrosc. Radiat. Transfer **29**, 465 (1983).